Published in final edited form as:
Neuroscience. 2012 December 13; 226: 165–177. doi:10.1016/j.neuroscience.2012.09.028.

PERIAQUEDUCTAL GRAY NEUROPLASTICITY FOLLOWING CHRONIC MORPHINE VARIES WITH AGE: ROLE OF OXIDATIVE STRESS

Dusica Bajic[a,b,1], **Charles B. Berde**[a,b], and **Kathryn G. Commons**[a,b]

[a]Department of Anesthesiology, Perioperative and Pain Medicine, Boston Children's Hospital, Boston, Massachusetts, USA

[b]Department of of Anæsthesia, Harvard Medical School, Boston, Massachusetts, USA

Abstract

The development of tolerance to the antinociceptive effects of morphine has been associated with networks within ventrolateral periaqueductal gray (vlPAG) and separately, nitric oxide signaling. Furthermore, it is known that the mechanisms that underlie tolerance differ with age. In this study, we used a rat model of antinociceptive tolerance to morphine at two ages, postnatal day (PD) 7 and adult, to determine if changes in the vlPAG related to nitric oxide signaling produced by chronic morphine exposure were age-dependent. Three pharmacological groups were analyzed: control, acute morphine, and chronic morphine group. Either morphine (10 mg/kg) or equal volume of normal saline was given subcutaneously twice daily for 6 ½ days. Animals were analyzed for morphine dose-response using *Hot Plate* test, and for the expression of several genes associated with nitric oxide metabolism was evaluated using rtPCR. In addition, the effect of morphine exposure on immunohistochemistry for Fos, and nNOS as well as nicotinamide adenine dinucleotide phosphate diaphorase (NADPH-d) reaction at the vlPAG were measured. In both age groups acute morphine activated Fos in the vlPAG, and this effect was attenuated by chronic morphine, specifically in the vlPAG at the level of the laterodorsal tegmental nucleus (LDTg). In adults, but not PD7 rats, chronic morphine administration was associated with activation of nitric oxide function. In contrast, changes in the gene expression of PD7 rats suggested superoxide and peroxide metabolisms may be engaged. These data indicate that there is supraspinal neuroplasticity following morphine administration as early as PD7. Furthermore, oxidative stress pathways associated with chronic morphine exposure appear age-specific.

Keywords

c-fos; Fos; nitric oxide; nNOS; opioid tolerance; periaqueductal gray

[1]**Corresponding Author**: **Dusica Bajic, MD, PhD**, Department of Anesthesiology, Perioperative and Pain Medicine, Boston Children's Hospital, Bader 3, 300 Longwood Avenue, Boston, MA 02115, Tel: 617-355-7737, Fax: 617-730-0894, dusica.bajic@childrens.harvard.edu.
[1]Permanent address

CONFLICT OF INTEREST STATEMENT
There are no conflicts of interest.

1. INTRODUCTION

Opioids, including morphine, are among the most effective treatments for postsurgical and cancer pain. Unfortunately, prolonged administration of morphine leads to the development of tolerance to analgesia, as evidenced by increased dosage requirements to maintain pain control. Moreover, age has an important effect on the development of tolerance (see review by Anand et al. (Anand et al., 2010)). However, differences in supraspinal neuroplasticity following chronic morphine administration with age remain poorly defined and understood. Considering the routine use of morphine infusions and the high incidence (35–57%) of antinociceptive tolerance in pediatric intensive care units (Katz et al., 1994, Fonsmark et al., 1999, Anand et al., 2010), elucidating the ontogeny of supraspinal chronic morphine effects is of current clinical interest.

The midbrain ventrolateral periaqueductal gray (vlPAG) is a major supraspinal site of systemic morphine's antinociceptive actions (Jensen and Yaksh, 1986, Morgan et al., 1998, Lane et al., 2005). It is also critical for the development of antinociceptive tolerance to morphine in the adult rat (Jacquet and Lajtha, 1976, Siuciak and Advokat, 1987, Tortorici et al., 1999, 2001, Lane et al., 2004, 2005, Morgan et al., 2006). The vlPAG contains neuronal isoform of nitric oxide synthase (nNOS) within cholinergic neurons that comprise the laterodorsal tegmental nucleus (LDTg) (McHaffie et al., 1991, Onstott et al., 1993, Rodrigo et al., 1994, Gotti et al., 2005). It is known that nNOS is responsible for the production of nitric oxide and not only plays an important role in morphine's acute effects (Mao, 1999, Mayer et al., 1999, Zhu and Barr, 2001b) but has also been implicated in the development of antinociceptive tolerance to morphine (Babey et al., 1994, Kielstein et al., 2007). Mice with a genetic deficiency of nNOS have significantly attenuated antinociceptive tolerance to morphine (Heinzen and Pollack, 2004a), while nNOS inhibitors have been reported to attenuate antinociceptive tolerance in adult rodents (Herman et al., 1995, Xu et al., 1998). However, it is not known if systemic morphine acts at the level of the vlPAG in the newborn rat. It is also poorly understood whether chronic morphine administration modifies supraspinal expression of nNOS or related genes in the vlPAG in either the adult or developing brain.

In this report, we focused our investigation on age-dependent changes as well as on the possible role of nNOS-expressing neurons of the vlPAG in mediating the effects of chronic morphine treatment. We hypothesized that chronic morphine exposure would be associated with neuroplasticity at the vlPAG as early as PD7, and that it would involve upregulation of nitric oxide. Specifically, the objective of the study was to identify changes in oxidative stress-related gene expression and the possible anatomical correlates within the vlPAG following chronic morphine administration. We utilized a model of antinociceptive tolerance to morphine in newborn rats previously described by Barr's group (Jones and Barr, 1995, Zhu and Barr, 2003). Finally, behavioral experiments were performed to confirm the development of antinociceptive tolerance to morphine using Hot Plate test in both adult and PD7 rats.

2. EXPERIMENTAL PROCEDURES

2.1. Animal Care and Use

Pregnant (day 18) Sprague-Dawley rats were derived from Sasco (Charles River Laboratories International, Inc., Wilmington, MA) were handled for several days before parturition and checked at 9 AM and 5 PM daily. Pups found at either time were termed 0 days of age, and were subsequently used for experiments at PD7. Male rats (250 g; average age PD57 according to the supplier) were purchased from the same source. Adult male rats were housed in groups of two or three, while each litter was in a separate cage. Animals

were maintained on a 12 hours light/dark cycle, and food and water were given ad libitum. The Institutional Animal Care and Use Committee at Children's Hospital Boston approved the experimental protocols for the use of vertebrate animals in this study. Experiments were conducted according to the United States Public Health Service Policy on Humane Care and Use of Laboratory Animals and the Guide for the Care and Use of Laboratory Animals (NIH Publications No. 80-23, revised 1996). All efforts were made to minimize the number of animals used and their discomfort.

2.2. Pharmacological Treatment

Morphine tolerance was induced following similar methods originally described by Jones and Barr (Jones and Barr, 1995). We used subcutaneous (sc) injections to minimize nociceptive experience from intraperitoneal (ip) drug administration. Specifically, animals received twice-daily sc injections for 6 days (9 AM and 5 PM) and received the last sc injection on the morning of the 7th day. Injections were done using 30 g needles (Becton Dickinson and Co., Franklin Lakes, NJ) in adult rats, while 10 μl and 100 μl Hamilton syringes (Hamilton Company, Reno, NV) were used for pups. Morphine sulfate (10 mg/kg; Baxter Healthcare Corp., Deerfield, IL) or equal volume of NS was administered in the sc area of the upper or lower back. Experimental groups included: **control group** that received only normal saline (NS) injections for 6 ½ days, **acute morphine group** that received NS except for the last injection on the morning of the 7th day when morphine was administered, and **chronic morphine group** that received only morphine for 6 ½ days. The first day of injections for pups occurred at PD1. Each litter had between 9 and 12 pups that were assigned to each of the pharmacological groups. Pups from both sexes were included since gender does not contribute to the degree of antinociceptive tolerance in neonatal rats (Thornton and Smith, 1997, Thornton et al., 1997).

2.3. Behavioral Experiments for Tolerance Assessment

The *Hot Plate* test was used to confirm the development of antinociceptive tolerance to morphine. A separate group of animals (n=6–7/pharmacological group/age) was used for behavioral testing to minimize nociceptive testing interference with measures of the sensitive neuroanatomical marker (Fos). We used a modified *Hot Plate* test (Masters et al., 1993) (T 56°C and 12 s cutoff latency) to measure distal 2/3 hindpaw withdrawal latency (in seconds) in adult rats, and the parameters for *Hot Plate* test are described in a study by Zhu and Barr (Zhu and Barr, 2001a) for PD7 rat (T 49°C and 20 s cutoff latency). Testing was done in the afternoon of the 7th day 20 minutes following each drug administration. After adaptation baseline trials, and trials following injection of NS, each rat was injected with a low dose of morphine (0.1 mg/kg sc). Thirty minutes later, the rats were re-tested and injected with the next dose of morphine that was increased in logarithmic manner with a starting dose of 0.1 mg/kg and an ending dose of 10 mg/kg, and increments of approximately half a log unit (such that each animal received 0.1, 0.3, 1, 3, and 10 mg/kg of morphine sequentially). Withdrawal latency of the hindpaw of each animal was measured 3 times on both sides after each drug injection (with 10 s pause interval) and the final withdrawal latency value was averaged among 6 recordings. In no case was there tissue damage. An individual blinded to the treatment group performed behavioral testing. *Hot Plate* data are presented as a percentage of maximum possible effect (%MPE=[Test Latency–Baseline Latency]/[Cutoff Time–Baseline Latency] ×100) ± SD, according to the method used by Harris and Pierson (Harris and Pierson, 1964).

2.4. Quantitative Gene Expression Analysis

We analyzed gene expression in two groups: **control group**, and **chronic morphine group** at two different ages. A replicate and pooling strategy was devised to minimize variance

cause by litter effects, the dissections themselves and other technical factors. For adults, tissue from 5 individuals was pooled for each treatment group and PCR replicate; there were 4 replicates such that a total for 40 adult rats were used. For P7 rats, the progeny from 3 litters were used for each PCR replicate. For each litter, pups were equally divided between saline or morphine treatment groups. Tissue derived from all the pups receiving the same treatment from the three litters were pooled for a single PCR replicate. The PCR analysis was repeated three times, thus we used total 9 litters (64 individual pups). One hour following the last injection on the morning of the 7th day, animals were deeply anesthetized with sodium pentobarbital 100 mg/kg ip and decapitated. Brains were removed, and coronal tissue blocks containing the ventral periaqueductal gray (PAG) at the level of the inferior colliculus (which included vlPAG, LDTg, and dorsal raphe nucleus; Fig. 1B), were dissected on ice. Tissue blocks corresponded to distances from Bregma of −7.64 to −9.16 according to the adult rat brain atlas (Paxinos and Watson, 1998). We dissected 26 ± 18 mg of the ventral PAG tissue per individual adult brain (n=40) and 13.5 ± 3 mg per individual PD7 brain (n=64). Tissue blocks from animals of the same group (n=5 animals/group) were collected and homogenized in 1 ml of Trizol Reagent (Life Technologies Corp., NY) for total RNA isolation using the phenol-chloroform method (Chomczynski and Sacchi, 1987), followed by the addition of 0.2 ml chloroform per 1 ml Trizol used. After incubation for 3 minutes at room temperature, samples were centrifuged at 11,000 g for 15 minutes at 4°C. The upper aqueous phase was transferred to another vial, and RNA was precipitated by adding 1 ml glycogen (Invitrogen, CA) and 0.5 ml isopropyl alcohol (Sigma, St. Louis, MO) per 1 ml Trizol used. After incubation of samples for 10 minutes at room temperature, separation of RNA was accomplished by centrifugation at 11,000 g for 15 minutes at 4°C. Pellets containing total RNA were washed once with 1 ml of 75% ethanol centrifuged at 7,500 g for 5 minutes at 4°C. After that, pellets containing washed RNA were dried for 3 minutes at room temperature, and then dissolved in RNAse-free water (50 ml water per 100 mg brain tissue homogenized). Samples were aliquoted and stored at −80°C. The RNA yield was evaluated in all the samples by analyzing the spectrophotometric ratios $_{260/280}$ using a Nanodrop 2000c Spectrophotometer (ThermoScientific, West Palm Beach, FL). Specifically, average yield of total RNA (± SD) from ventral PAG was 1.8 ± 0.2 μg/μl (n=4 replicates/2 groups) and 3.23 ± 0.4 μg/μl (n=3 replicates/2 groups) from adult and PD7 rat, respectively. RNA integrity was corroborated using 2% agarose gels with ethidium bromide (3 ml/50 ml TRIS) and visualized in a UV transilluminator, showing two main bands corresponding to 18S and 28S rRNAs (data not shown). Samples containing a minimum of 5 μg of RNA (at a concentration greater than 0.5 μg/μl) were sent in dry ice to SABiosciences™ (Frederick, MD) for quantitative PCR analysis using the *Rat Nitric Oxide Signaling Pathway PCR Array* (PARN-062; SABiosciences™-a QIAGEN company). For the list of all 84 genes in the Array (PARN-060), refer to SABiosciences™ website.

2.5. Anatomical Experiments

For anatomical experiments, a total of 15 adult animals (n=5/group) and 13 pups (n=4–5/group) were used in 3 experimental groups: control, acute morphine, and chronic morphine groups. Animals were anesthetized and transcardially perfused on PD7 and PD65 (estimated). The time point selected for perfusion on the 7th day of pharmacological treatment was 2 hours after the last sc injection. This time point was selected because antinociceptive effects following systemic administration of morphine in rats peak at around 60 minutes. In addition, Fos protein expression generally peaks at 1 hour and disappears by 3–4 hours (Herdegen and Leah, 1998) after either short or continuous stimulus. Therefore, a 1 hour delay for maximum morphine effect, followed by an hour delay for subsequent maximal Fos expression. Experimental groups were matched and individuals from different groups were processed in parallel. Specifically, after anesthesia, adult animals were perfused through the ascending aorta with 50 ml of normal saline, followed by 250 ml of 4%

paraformaldehyde in 0.1M phosphate buffer (PB, pH 7.4, room temperature). Rat pups were perfused with only 100 ml of 4% paraformaldehyde in 0.1M PB solution. Brains were removed and stored in the same fixative solution overnight (4°C) before cryoprotection in 30% sucrose solution in 0.1M PB for at least 48 hours. Subsequently, brains were frozen and 40 μm coronal sections were cut on a freezing microtome. Free-floating sections were collected in 0.1M PB in saline and subsequently processed for: (1) Fos and nNOS immunolabeling, and (2) NADPH-d histochemistry reaction.

2.5.1. Fos and nNOS Immunocytochemistry—Primary and secondary antisera were diluted in 0.1M PB with normal saline, 0.3% Triton X-100, 0.04% bovine serum albumin, and 0.1% sodium azide. Brain sections were incubated in primary antibodies for 2 days at 4°C, and subsequently in secondary antibodies for 1 to 2 hours at room temperature. Sections were rinsed in 0.1M PB in saline (3 times for 10 minutes) in between immunocytochemical processing. Fos immunoreactivity was detected by incubating sections in rabbit polyclonal anti-Fos antisera (Oncogene, Cambridge, MA) diluted 1:10,000, while a mouse monoclonal antibody to nNOS (diluted 1:5000; NOS1 (A-11) sc-5302; Santa Cruz Biotechnology Inc., Santa Cruz, CA) was used for nNOS neurons labeling. Secondary antiserum for Fos was raised in donkey and conjugated to Cy3 (red fluorophore; Jackson ImmunoResearch Labs, Inc., West Grove, PA). Secondary antisera raised in donkey (anti-mouse) were conjugated to Alexa Fluor^{R} 488 (green fluorophore; Invitrogen Corp., Carlsbad, CA). All secondary antisera were diluted to 1:200. Immunolabeling with anti-Fos antisera produces characteristic nuclear staining consistent with the role of the protein in transcription, while nNOS labeling leads to neuronal body staining. Finally, sections were rinsed in 0.1M PB in saline solution prior to mounting on slides in 0.05M PB. After drying, mounted sections were coverslipped with 90% glycerol solution.

2.5.2. Nicotinamide Adenine Dinucleotide Phosphate-Diaphorase (NADPH-d) Histochemical Reaction—Previous studies have demonstrated that nNOS and NADPH coexist in cellular profiles of the vlPAG (Xu and Hokfelt, 1997, Simpson et al., 2003, Okere and Waterhouse, 2006a), and that NADPH-d is an index of nNOS activity (Hope et al., 1991). Thus, 1/4 of free-floating sections through the LDTg were collected and processed for NADPH-d reaction following a modified protocol by Okere and Waterhouse (Okere and Waterhouse, 2006c, b). Tissue sections were incubated in 10 ml of 0.1M PB solution containing 4 mg nitroblue tetrazolium (Sigma, St. Louis, MO, USA), 2 mg reduced β-NADPH-d (Sigma, St. Louis, MO, USA) and 0.03% Triton X-100 for 30–35 min in a 40°C water bath. Rinsing sections in 0.1M PB buffer stopped the reaction. Sections were mounted on superfrosted glass slides in 0.05M PB, air-dried, cleared in ascending alcohol solutions (35%, 50%, 70%, 95%, 100%) for one minute each prior to dehydration in xylene for 3 minutes twice. Finally, sections were air-dried prior to permanently coverslipping with Permount (Fisher Scientific, Pittsburg, PA, USA).

2.5.3. Mapping and Cell Counts—The analysis of all neurons was done using a fluorescent/brightfield microscope (Olympus IX81; Olympus America Inc. Melville, NY, USA) equipped with a camera and digital microscopy software (Slidebook v4.2, Olympus). For Fos and nNOS quantitative analysis, we divided the ventral PAG along the rostrocaudal axis into 3 areas (Fig. 1): **Level 1 –** caudal region that encompasses central gray at the level of the rostral locus coeruleus (Plates 56–59 according to the adult rat brain atlas (Paxinos and Watson, 1998)), **(2) Level 2 –** mid region at the level of the inferior colliculus where serotonergic neurons comprise mid dorsal raphe nucleus (corresponding to Plates 53–55), and **(3) Level 3** – rostral region at the level of the superior colliculus where rostral dorsal raphe nucleus is located (corresponding to Plates 48–52). In the first two areas, nNOS immunoreactive neurons are of type I (strongly immunoreactive larger neurons) comprising

LDTg whereas in the third region, they are of type II (lightly labeled and smaller in size) that are located in the dorsal raphe nucleus (Onstott et al., 1993, Rodrigo et al., 1994). Both Fos immunolabeled nuclei and nNOS immunoreactive neurons were counted bilaterally only in the boundaries of the ventral PAG as illustrated by Fig. 1. For each rat, an average of 3–5 coronal sections representing each of these areas bilaterally were photographed. For each area, a minimum of 5 adult rats and 4–5 PD7 rats per pharmacological group contributed to the mean number of counted profiles (density/section). Double-labeled neurons were manually enumerated from photographs by visualizing the individual and merged images of each fluorophore. nNOS immunolabeled neurons were considered Fos-positive if the nucleus was entirely filled with labeling for Fos, and the surrounding cell body and proximal dendrites filled with labeling for nNOS, as visualized by two different fluorophore (red and green, respectively). To confirm that Fos was detectable using immunofluorescence, the sections analyzed were first examined for Fos immunolabeling in other brain areas besides those of our interest, for all treatment groups. An observer blind to the treatment group counted single and dual-immunolabeling of individual profiles.

2.5.4. Intensity of Labeling per Individual Neuron—Bilateral pictures of the LDTg were taken uniformly with 10× magnification lens at 400 ms exposure (for nNOS fluorescent microscopy) and 1000 ms (for NADPH-d brightfield microscopy) among different brains. Note that complementary sets of brain tissue per age were processed simultaneously and photographed with the same exposure time to minimize inter-assay variability. Average intensity per individual neuron of either nNOS-immunoreactive labeling or NADPH-d reaction product was calculated based on analysis of intensity labeling in 5 individual neurons per picture of LDTg (total 6 pictures/brain, n=5–6 brains/treatment group). Background labeling intensity was subtracted from the total intensity of nNOS labeling/NADPH-d reactivity in each individual neuron that was analyzed. Furthermore, for NADPH-d labeling, we counted the number of lightly labeled (light), intensely reactive (dark), as well as the total number of NADPH-d reactive neurons in each picture. This was done by grading individually neurons as either dark or light, where a 'dark' neuron was defined by either (1) black cytoplasmic reaction or (2) an intense reaction that obscured characteristics of a neuronal nucleus. In constrast, light neurons were characterized by gray cytoplasm and easily detectable nucleus. This analysis was also blinded as per pharmacological treatment group.

2.6. Statistical Analyses

For gene expression analysis, the effect of morphine treatment at each age was analyzed using unpaired two-tailed Student t-test, and genes with a $p<0.10$ were reported. For (1) average *Hot Plate* withdrawal effect (%MPE), (2) mean density of immunohistochemical profiles (# of immunolabeled profiles/section/brain), and (3) average intensity of nNOS immunolabeling or NADPH-d reaction per individual neuron in LDTg, for each age we used one-way analysis of variance (ANOVA) for treatment effect with a Tukey HSD post-hoc test. A p-value less than 0.05 was considered statistically significant.

3. RESULTS

3.1. Behavioral Analysis of Antinociceptive Tolerance with Age

To validate the model of chronic morphine exposure in adult and PD7 rats (Barr and Wang, 1992, Zhu and Barr, 2003), we performed *Hot Plate* testing to examine the development of antinociceptive tolerance. Both PD7 and adult rats developed antinociceptive tolerance after chronic morphine treatment, as indicated by decreased antinociceptive effect (Fig. 2).

3.2. Gene Expression Changes in the Ventral Periaqueductal Gray with Treatment

We analyzed gene expression differences following chronic morphine treatment when compared to control (chronic NS treatment) at each age (Fig. 3). In the adult rat, chronic morphine treatment was associated an upregulation of *c-fos* (1.76 fold, p=0.03) and *noxa-1* (2.52 fold, p=0.09) genes. Although *NOS1* gene expression increased 1.6 fold (60%) in the adult rat following chronic morphine treatment in comparison to NS control, it was not significant (p=0.32). In PD7 rats, chronic morphine treatment was associated with an upregulation of *noxo1* (1.48 fold, p=0.08), *MPO* (2.33 fold, p=0.04), and *Txnip* (1.77 fold, p=0.01) genes related to superoxide and hypochlorous acid production, and antioxidant role of thioredoxin protein, respectively. Finally, three additional genes related to nitric oxide signaling appeared changed following chronic morphine treatement in PD7 rat, and included *Egr1* (1.8 fold, p=0.02), *Rprm* (−1.13 fold, p=0.07) and *Idh1* (−1.16 fold, p=0.09).

3.3. Density of Fos Immunoreactive Nuclei

3.3.1. Fos Density After Acute MorphineTreatment—Distribution of baseline Fos–immunolabeled cells in vlPAG of control groups is similar at both ages (Fig 4 and 4A’). Furthermore, acute morphine leads to Fos activation in the vlPAG of adult and PD7 rats. We confirm previous observations that acute morphine activates Fos expression in the vlPAG of adult rats (Loyd et al., 2007) (Fig. 5A’). In the PD7 rat, acute morphine administration also activated Fos in the vlPAG ($p<0.01$ at Level 2; Fig.5A), but not as broadly along the rostral-caudal extent as seen in adults (Fig. 5A and A’) nor to the same magnitude (Fig. 4B and B’).

3.3.2. Fos Density After Chronic MorphineTreatment—We also examined if Fos expression produced by acute morphine was attenuated after previous chronic exposure. Chronic morphine exposure led to a region-specific attenuation of Fos density in the vlPAG of both PD7 ($p<0.01$; Fig. 5A) and adult rats ($p<0.05$; Fig. 5A’) when compared to the acute morphine group. This effect was specific to a selective region of the vlPAG at the level of the inferior colliculus where cholinergic neurons that contain nNOS and comprise LDTg nucleus are located (area illustrated in Fig. 1B and Fos distribution in Fig. 4).

3.4. Analysis of Neuronal Nitric Oxide Synthase Immunoreactive Neurons

3.4.1. Density of nNOS Neurons with Morphine Treatment—We also analyzed the number of nNOS immunoreactive neurons at three different levels along the rostrocaudal axis of the ventral PAG (Fig. 1A–C). There was no change in the average density of nNOS neurons in any of the analyzed anatomical areas following either acute or chronic morphine administration in either adult or PD7 rat (Fig. 6A and A’). Furthermore, only a few double-labeled nNOS neurons with Fos immunoreactivity were identified. Measured density of double-labeled nNOS neurons with Fos in the adult was not statistically different along the rostrocaudal axis in any of the treatment groups and was negligible in the PD7 rat (Fig. 6B and B’).

3.4.2. Intensity of nNOS Immunoreactivity per Individual Neuron—Since there were no differences in the density of nNOS immunoreactive neurons with morphine treatment, but there were potential changes in *Nos1* gene transcription, we examined the average intensity of nNOS immunolabeling per individual neuron. This analysis revealed that the average intensity of nNOS immunoreactive labeling per individual neuron was different among the three treatment groups only in adult and not in PD7 rats (Fig. 6C and C’). More specifically, average intensity of nNOS immunoreactive labeling per individual neuron of adult LDTg significantly increased 26% in the group that received chronic morphine treatment when compared to control ($p<0.01$) and acute morphine ($p<0.01$) groups

(Fig. 6C'). However, this was specific to adults and no differences were found in PD7 (Fig. 6C).

3.4.3. Intensity of NADPH-d Reaction per Individual Neuron—To examine if changes in nNos immunoreactivity reflected increases in enzymatic activity, we also processed sections for NADPH-d reaction (Fig. 7). The average total number of NADPH-d stained neurons/adult brain ± SD (878.33 ± 136.33) was not different among different pharmacological groups. However, the percentage ± SD of intensely labeled (dark) neurons/section/brain was significantly higher in chronic morphine group in comparison to both control and acute morphine groups (Fig. 7A–C). Similarly, the percentage ± SD of lightly labeled NADPH-d neurons/section/brain was significantly lower in chronic morphine group (39.83% ± 12.49) in comparison to both control and acute morphine groups. Finally, average intensity of NADPH-d reaction per individual neuron of adult LDTg significantly increased 44% in the group that received chronic morphine treatments when compared to control and acute morphine groups (Fig. 7D). Similar analysis of the LDTg in the PD7 rats showed no significant difference in either percent of lightly reactive ($p=0.09$), percent of dark NADPH-d neurons/section/brain ($p=0.32$), or average intensity of NADPH-d reaction per individual neuron ($p=0.59$) among three different treatment groups (not shown).

4. DISCUSSION

In the present study, we examined the effects of systemic acute and chronic morphine administration on markers of neuroplasticity in the vlPAG at two different ages. In both adult and PD7 rats, acute morphine activates Fos and this effect is attenuated after chronic morphine administration. This effect illustrates that even at young PD7 age, morphine exposure has effects supraspinally, and chronic exposure results in neuroplasticity that changes these effects. In adults, this was associated with the up-regulation of genes associated with Fos (*Fos*) and NADPH oxidase (*noxa1*). However, similar changes do not appear to occur in the PD7 rat; rather there are gene expression changes that suggest alterations in superoxide (*noxo1*) and peroxide metabolism (*MPO*). Therefore, although both acute and chronic morphine exposure appear to impact the vlPAG at both ages, adaptive responses related to oxidative stress exhibit distinct characteristics.

4.1. Methodological Considerations

PCR is a sensitive method for detection of RNA expression levels in selected tissue. We used a pooling strategy combined with biological and technical replication to optimize this approach. Pooling was used in particular to minimize individual variation, litter effect, and technical variation caused by the dissections themselves. While our statistical approach was subject to false-positive error, relatively few differences in gene expression were detected. In order to confirm some of these results and understand the relevant neuroanatomy, we combined PCR with neuroanatomical approaches. We used Fos immunolabeling, which is easily detected and quantified, and has been used to understand the effects of analgesics and drugs of abuse including morphine (Chang et al., 1988, Liu et al., 1994). However Fos-immunolabeling can be vulnerable to errors if the amount of activation required to initiate expression of *c-fos* is different for different types of neurons (Dragunow and Faull, 1989). The latter might explain the lack of detectable Fos expression within nNOS-containing neurons in this study. In addition, it is worth considering that the NADPH-d reaction intensity could vary due to changes in fixation and tissue processing parameters (Spessert and Layes, 1994, Buwalda et al., 1995, Gonzalez-Hernandez et al., 1996). However, previous studies have shown that (1) extended fixation with 4% formaldehyde (that was used in our study) is necessary to inactive all other diaphorases except for NOS (Matsumoto et al., 1993), (2) that the amount of formazan blue produced at any given time reflects NOS

activity at the time of fixation (Hope et al., 1991, Morris et al., 1997), and (3) that the cellular intensity of NADPH-d reaction is subject to pharmacological manipulation (Gonzalez-Hernandez et al., 1996, Okere and Waterhouse, 2006c, b, a). Therefore, experimental and control animals were simultaneously processed under identical conditions throughout the handling, drug injections, perfusion, tissue preparation, NADPH-d histochemistry, and microscopy under the same light exposure, to reduce inter-experiment variability to the barest minimum.

4.2. Neuroplasticity in the vlPAG following Chronic Morphine Administration

Pharmacological studies have implicated vlPAG as an essential brain region mediating antinociceptive tolerance to chronic morphine administration (Lane et al., 2004). Furthermore, this is due to a direct effect of morphine in the vlPAG, as experiments have shown that in the adult rat, morphine's actions within the vlPAG are sufficient to produce antinociceptive tolerance (Lane et al., 2005). Previous study by Loyd et al. (Loyd et al., 2008) reported attenuation of Fos activation of adult spinally projecting neurons following chronic morphine administration without any change in the total number of Fos. Factors that might explain the discrepancy with the current report include differences in animal treatment (tracer injection surgeries vs. naïve animals in our study), methods of anatomical quantification (the caudal vlPAG region was divided into three separate regions in our study), or pharmacological treatment (chronic morphine administration for 3 ½ days vs. 6 ½ days in our study). However, our results are consistent with Loyd et al. in providing evidence for tolerance to morphine's effects at the level of vlPAG networks. Furthermore, our results show this effect is detected as early as PD7. The latter novel finding brings new light into supraspinal opioid effects of developing rat brain. It is known that morphine and other opioid agonists are effective analgesics during the early neonatal period (Kehoe and Blass, 1986a) due to the presence of spinal opioid receptors at birth (Rahman and Dickenson, 1999). Although it is clear that descending inhibitory mechanisms are still not completely functional until the third week of life (Nandi and Fitzgerald, 2005, Fitzgerald and Walker, 2009), several studies reported that morphine injected into the ventricle or directly into the vlPAG produces antinociception as early as PD7 (Kehoe and Blass, 1986b, Barr et al., 1992, Tive and Barr, 1992, Tseng et al., 1995). Thus, our data confirm that acute morphine has effects on supraspinal networks of vlPAG as early as PD7, and moreover, that chronic morphine exposure is associated with plasticity of vlPAG with development of antinociceptive tolerance.

4.3. Ontogeny of Oxidative Stress Gene Expression in Ventral PAG with Morphine

We report that selective, oxidative stress-related genes are differentially expressed following chronic morphine administration in a rat model at two different ages: newborn (PD7) and adult. In contrast to nNOS, the enzyme responsible for production of nitric oxide, Nox1 and Nox4 generate and release intracytoplasmic superoxide (O_2^-) and extracellular hydrogen peroxide (H_2O_2), respectively (Ambasta et al., 2004, Martyn et al., 2006, von Lohneysen et al., 2008). Furthermore, Noxa1 together with Noxo1 are key regulatory subunits of the NADPH oxidase Nox1 known for producing O_2^- constitutively at low levels (Banfi et al., 2003, Takeya et al., 2003). According to our novel gene expression analysis, O_2^- (*noxo1*) may be upregulated by opioid exposure in the ventral PAG of the PD7 rat but not nitric oxide (*Nos1*). Furthermore, *MPO* gene may be upregulated following chronic morphine administration in PD7 rat. This gene is responsible for expression of myeloperoxidase, an enzyme that produces hypochlorous acid (HOCl) from H_2O_2 (van der Veen et al., 2009). Taken together, these changes could suggest changes in superoxide and peroxide metabolisms may be engaged at younger ages. In addition, expression of transcription factors differed at each age with Fos expression increased in adults, and Egr1 increased in PD7 rats. While our statistical criteria may include false-positive findings, these data would

suggest that there are age-dependent transcriptional changes within cells in the ventral PAG as a result of opioid exposure.

4.4. Nitric Oxide Upregulation Associated with Chronic Morphine Administration

Recent evidence indicates that nitric oxide is a key mediator of antinociceptive tolerance since increased nitric oxide production results in an enhanced rate and extent of development of antinociceptive tolerance to morphine (Babey et al., 1994, Xu et al., 1998, Heinzen and Pollack, 2004b, Kielstein et al., 2007). Blockade of nNOS by a selective nNOS inhibitor attenuates antinociceptive tolerance to morphine in the adult rats (Herman et al., 1995, Xu et al., 1998). It was also reported that repeated morphine administration increases NOS biosynthesis in the rat spinal cord, as demonstrated by in situ hybridization and immunohistochemical techniques (Machelska et al., 1997). Our results complement those findings by demonstrating dramatic increase in NADPH-diaphorase activity in adults, which may be due to both an increase in expression per cell as well as post-translational regulation that could increase nNOS enzymatic activity.

4.4.1. Fos-Independent nNOS Activation in the LDTg With Chronic Morphine—

Although there is an increase in nNOS enzymatic activity, these neurons do not tend to exhibit Fos after acute morphine exposure. This suggests that nNOS neurons do not comprise descending efferent pathways mediating opioid effects from the vlPAG, which are indirectly activated by acute morphine exposure (see reviews (Basbaum and Fields, 1984, Fields et al., 2006)). Our preliminary results indicate that mu-opioid receptors are located on nNOS neurons in the adult rat but not PD7 rat (D. Bajic and K.G. Commons, unpublished observations). While many nNOS neurons are known to be cholinergic (Sugaya and McKinney, 1994, Cork et al., 1998), nNOS could potentially be present in GABAergic neurons, since it is known that mu- opioid receptors are present on the GABAergic neurons in the vlPAG (Commons et al., 2000). Maturation of GABAergic neurons and GABA immunoreactive terminals in the vlPAG does not occur until the second postnatal week and is not fully established until PD30 (Barbaresi, 2010). The relationship between maturation of GABAergic neurons in the vlPAG and nNOS may be interesting to further understand with respect to the changing mechanisms of opioid actions with age.

Furthermore, studies by Waterhouse group have demonstrated that stress (restraint) and painful stimuli (capsaicin) lead to the upregulation of NOS activity (as demonstrated by increased total NADPH-d staining intensity) in the LDTg, without a concomitant change in the mean number of neurons (Okere and Waterhouse, 2006c, b, a). This is in agreement with our report of a statistically significant increase in the average intensity of both nNOS immunohistochemistry and NADPH-d staining intensity per individual nNOS neuron in the vlPAG of the adult rat. Thus, it is possible that an increased release of nitric oxide locally in the LDTg of the vlPAG following chronic morphine administration may serve to either inhibit output neurons, or activate local GABA interneurons (Shin et al., 1997, Yang et al., 2007). Either effect would lead to a decreased output of efferent vlPAG neurons that may, in part, contribute to antinociceptive tolerance to morphine in adult rat.

In addition to its local effect on the vlPAG circuitry, increased nNOS activity within the LDTg following chronic administration of morphine may also have effects along its efferent projections. Cholinergic neurons of LDTg/pedunculopontine tegmentum provide the only known cholinergic input to the ventral tegmental area (Oakman et al., 1995, Holmstrand and Sesack, 2011). Our preliminary data indicate that 98% of cholinergic neurons comprising the LDTg are colocalized with nNOS in the adult rat as previously reported (Blottner et al., 1995). Therefore, up-regulated nitric oxide following chronic morphine administration might also be involved in the modulation of motivated behavior and reward pathways (see reviews (Lester et al., 2010, Mark et al., 2011)). Finally, Usunoff et al. (Usunoff et al., 1999)

reported that ~25% of rat LDTg/pedunculopontine tegmental projection neurons target the ventrobasal thalamus and stain positively for NADPH-d (as index of NOS). This suggests an additional role of nitric oxide in thalamic somatosensory processing following chronic morphine administration. Future studies should elucidate functional significance of upregulated nNOS on specific consequences of chronic morphine exposure in addition to antinociceptive tolerance, such as sensitization, place preference and dependence.

4.5. Conclusions

Chronic systemic morphine administration is associated with supraspinal neuroplasticity in the vlPAG as early as the PD7 in the rat. It involves oxidative stress mechanisms that differ with age. Nitric oxide is implicated in adult, while gene expression analysis implicates superoxide and hydrogen peroxide mechanisms to be associated with chronic morphine administration in the PD7 rat.

Acknowledgments

This work was supported by the Foundation for Anesthesia Education and Research (FAER), Endo Pharmaceuticals, and NIH R03 DA030874 (D.B.), Mayo Family Research Endowment Fund (C.B.B.), and NIH R01 DA021801 (K.G.C.). Authors would like to thank Drs. Mariano Soiza-Reilly and Jia-Ren Liu for technical expertise in molecular techniques, Dr. Sulpicio G. Soriano for the use of the equipment for the total RNA extraction, and Dr. Rani K. Vasudeva for help with NADPH-d reaction protocol.

ABBREVIATIONS

ANOVA	analysis of variance
Ct	cycle threshold
ip	intraperitoneal
sc	subcutaneous
LDTg	laterodorsal tegmental nucleus
NADPH-d	nicotinamide adenine dinucleotide phosphate diaphorase
NS	normal saline
nNOS	neuronal nitric oxide synthase (NOS1)
PAG	periaqueductal gray
PB	phosphate buffer
PD	postnatal day
PCR	polymerase chain reaction
vlPAG	ventrolateral periaqueductal gray
%MPE	percentage of maximum possible effect

LITERATURE CITED

Ambasta RK, Kumar P, Griendling KK, Schmidt HH, Busse R, Brandes RP. Direct interaction of the novel Nox proteins with p22phox is required for the formation of a functionally active NADPH oxidase. J Biol Chem. 2004; 279:45935–45941. [PubMed: 15322091]

Anand KJ, Willson DF, Berger J, Harrison R, Meert KL, Zimmerman J, Carcillo J, Newth CJ, Prodhan P, Dean JM, Nicholson C. Tolerance and Withdrawal From Prolonged Opioid Use in Critically Ill Children. Pediatrics. 2010; 125:1208–1225. [PubMed: 20457682]

Babey AM, Kolesnikov Y, Cheng J, Inturrisi CE, Trifilletti RR, Pasternak GW. Nitric oxide and opioid tolerance. Neuropharmacology. 1994; 33:1463–1470. [PubMed: 7532830]

Banfi B, Clark RA, Steger K, Krause KH. Two novel proteins activate superoxide generation by the NADPH oxidase NOX1. J Biol Chem. 2003; 278:3510–3513. [PubMed: 12473664]

Barbaresi P. Postnatal development of GABA-immunoreactive neurons and terminals in rat periaqueductal gray matter: a light and electron microscopic study. J Comp Neurol. 2010; 518:2240–2260. [PubMed: 20437526]

Barr GA, Miya DY, Paredes W. Analgesic effects of intraventricular and intrathecal injection of morphine and ketocyclazocine in the infant rat. Brain Res. 1992; 584:83–91. [PubMed: 1515954]

Barr GA, Wang S. Tolerance and withdrawal to chronic morphine treatment in the week-old rat pup. Eur J Pharmacol. 1992; 215:35–42. [PubMed: 1516648]

Basbaum AI, Fields HL. Endogenous pain control systems: brainstem spinal pathways and endorphin circuitry. Annu Rev Neurosci. 1984; 7:309–338. [PubMed: 6143527]

Blottner D, Grozdanovic Z, Gossrau R. Histochemistry of nitric oxide synthase in the nervous system. Histochem J. 1995; 27:785–811. [PubMed: 8575942]

Buwalda B, Nyakas C, Gast J, Luiten PG, Schmidt HH. Aldehyde fixation differentially affects distribution of diaphorase activity but not of nitric oxide synthase immunoreactivity in rat brain. Brain Res Bull. 1995; 38:467–473. [PubMed: 8665271]

Chang SL, Squinto SP, Harlan RE. Morphine activation of c-fos expression in rat brain. Biochem Biophys Res Commun. 1988; 157:698–704. [PubMed: 3144275]

Chomczynski P, Sacchi N. Single-step method of RNA isolation by acid guanidinium thiocyanate-phenol-chloroform extraction. Anal Biochem. 1987; 162:156–159. [PubMed: 2440339]

Commons KG, Aicher SA, Kow LM, Pfaff DW. Presynaptic and postsynaptic relations of mu-opioid receptors to gamma-aminobutyric acid-immunoreactive and medullary-projecting periaqueductal gray neurons. J Comp Neurol. 2000; 419:532–542. [PubMed: 10742719]

Cork RJ, Perrone ML, Bridges D, Wandell J, Scheiner CA, Mize RR. A web-accessible digital atlas of the distribution of nitric oxide synthase in the mouse brain. Prog Brain Res. 1998; 118:37–50. [PubMed: 9932433]

Dragunow M, Faull R. The use of c-fos as a metabolic marker in neuronal pathway tracing. J Neurosci Methods. 1989; 29:261–265. [PubMed: 2507830]

Fields, HL.; Basbaum, AI.; Heinricher, MM. Central nervous systems mechanisms of pain modulation. In: McMahon, SB.; Koltzenburg, M., editors. Textbook of Pain. Philadelphia, PA: Elsevier, Churchill Livingston; 2006. p. 125-142.

Fitzgerald M, Walker SM. Infant pain management: a developmental neurobiological approach. Nat Clin Pract Neurol. 2009; 5:35–50. [PubMed: 19129789]

Fonsmark L, Rasmussen YH, Carl P. Occurrence of withdrawal in critically ill sedated children. Crit Care Med. 1999; 27:196–199. [PubMed: 9934916]

Gonzalez-Hernandez T, Perez de la Cruz MA, Mantolan-Sarmiento B. Histochemical and immunohistochemical detection of neurons that produce nitric oxide: effect of different fixative parameters and immunoreactivity against non-neuronal NOS antisera. J Histochem Cytochem. 1996; 44:1399–1413. [PubMed: 8985132]

Gotti S, Sica M, Viglietti-Panzica C, Panzica G. Distribution of nitric oxide synthase immunoreactivity in the mouse brain. Microsc Res Tech. 2005; 68:13–35. [PubMed: 16208717]

Harris LS, Pierson AK. Some Narcotic Antagonists in the Benzomorphan Series. J Pharmacol Exp Ther. 1964; 143:141–148. [PubMed: 14163985]

Heinzen EL, Pollack GM. The development of morphine antinociceptive tolerance in nitric oxide synthase-deficient mice. Biochem Pharmacol. 2004a; 67:735–741. [PubMed: 14757173]

Heinzen EL, Pollack GM. Pharmacodynamics of morphine-induced neuronal nitric oxide production and antinociceptive tolerance development. Brain Res. 2004b; 1023:175–184. [PubMed: 15374743]

Herdegen T, Leah JD. Inducible and constitutive transcription factors in the mammalian nervous system: control of gene expression by Jun, Fos and Krox, and CREB/ATF proteins. Brain Res Brain Res Rev. 1998; 28:370–490. [PubMed: 9858769]

Herman BH, Vocci F, Bridge P. The effects of NMDA receptor antagonists and nitric oxide synthase inhibitors on opioid tolerance and withdrawal. Medication development issues for opiate addiction. Neuropsychopharmacology. 1995; 13:269–293. [PubMed: 8747752]

Holmstrand EC, Sesack SR. Projections from the rat pedunculopontine and laterodorsal tegmental nuclei to the anterior thalamus and ventral tegmental area arise from largely separate populations of neurons. Brain Struct Funct. 2011; 216:331–345. [PubMed: 21556793]

Hope BT, Michael GJ, Knigge KM, Vincent SR. Neuronal NADPH diaphorase is a nitric oxide synthase. Proc Natl Acad Sci U S A. 1991; 88:2811–2814. [PubMed: 1707173]

Jacquet YF, Lajtha A. The periaqueductal gray: site of morphine analgesia and tolerance as shown by 2-way cross tolerance between systemic and intracerebral injections. Brain Res. 1976; 103:501–513. [PubMed: 1252940]

Jensen TS, Yaksh TL. Comparison of antinociceptive action of morphine in the periaqueductal gray, medial and paramedial medulla in rat. Brain Res. 1986; 363:99–113. [PubMed: 3004644]

Jones KL, Barr GA. Ontogeny of morphine withdrawal in the rat. Behav Neurosci. 1995; 109:1189–1198. [PubMed: 8748967]

Katz R, Kelly HW, Hsi A. Prospective study on the occurrence of withdrawal in critically ill children who receive fentanyl by continuous infusion. Crit Care Med. 1994; 22:763–767. [PubMed: 8181283]

Kehoe P, Blass EM. Behaviorally functional opioid systems in infant rats: II. Evidence for pharmacological, physiological, and psychological mediation of pain and stress. Behav Neurosci. 1986a; 100:624–630. [PubMed: 3640642]

Kehoe P, Blass EM. Central nervous system mediation of positive and negative reinforcement in neonatal albino rats. Brain Res. 1986b; 392:69–75. [PubMed: 3011217]

Kielstein A, Tsikas D, Galloway GP, Mendelson JE. Asymmetric dimethylarginine (ADMA)-a modulator of nociception in opiate tolerance and addiction? Nitric Oxide. 2007; 17:55–59. [PubMed: 17625935]

Lane DA, Patel PA, Morgan MM. Evidence for an intrinsic mechanism of antinociceptive tolerance within the ventrolateral periaqueductal gray of rats. Neuroscience. 2005; 135:227–234. [PubMed: 16084660]

Lane DA, Tortorici V, Morgan MM. Behavioral and electrophysiological evidence for tolerance to continuous morphine administration into the ventrolateral periaqueductal gray. Neuroscience. 2004; 125:63–69. [PubMed: 15051146]

Lester DB, Rogers TD, Blaha CD. Acetylcholine-dopamine interactions in the pathophysiology and treatment of CNS disorders. CNS Neurosci Ther. 2010; 16:137–162. [PubMed: 20370804]

Liu J, Nickolenko J, Sharp FR. Morphine induces c-fos and junB in striatum and nucleus accumbens via D1 and N-methyl-D-aspartate receptors. Proc Natl Acad Sci U S A. 1994; 91:8537–8541. [PubMed: 8078918]

Loyd DR, Morgan MM, Murphy AZ. Morphine preferentially activates the periaqueductal gray-rostral ventromedial medullary pathway in the male rat: a potential mechanism for sex differences in antinociception. Neuroscience. 2007; 147:456–468. [PubMed: 17540508]

Loyd DR, Morgan MM, Murphy AZ. Sexually dimorphic activation of the periaqueductal gray-rostral ventromedial medullary circuit during the development of tolerance to morphine in the rat. Eur J Neurosci. 2008; 27:1517–1524. [PubMed: 18364026]

Machelska H, Ziolkowska B, Mika J, Przewlocka B, Przewlocki R. Chronic morphine increases biosynthesis of nitric oxide synthase in the rat spinal cord. Neuroreport. 1997; 8:2743–2747. [PubMed: 9295111]

Mao J. NMDA and opioid receptors: their interactions in antinociception, tolerance and neuroplasticity. Brain Res Rev. 1999; 30:289–304. [PubMed: 10567729]

Mark GP, Shabani S, Dobbs LK, Hansen ST. Cholinergic modulation of mesolimbic dopamine function and reward. Physiol Behav. 2011; 104:76–81. [PubMed: 21549724]

Martyn KD, Frederick LM, von Loehneysen K, Dinauer MC, Knaus UG. Functional analysis of Nox4 reveals unique characteristics compared to other NADPH oxidases. Cell Signal. 2006; 18:69–82. [PubMed: 15927447]

Masters DB, Berde CB, Dutta SK, Griggs CT, Hu D, Kupsky W, Langer R. Prolonged regional nerve blockade by controlled release of local anesthetic from a biodegradable polymer matrix. Anesthesiology. 1993; 79:340–346. [PubMed: 8342843]

Matsumoto T, Nakane M, Pollock JS, Kuk JE, Forstermann U. A correlation between soluble brain nitric oxide synthase and NADPH-diaphorase activity is only seen after exposure of the tissue to fixative. Neurosci Lett. 1993; 155:61–64. [PubMed: 7689718]

Mayer DJ, Mao J, Holt J, Price DD. Cellular mechanisms of neuropathic pain, morphine tolerance, and their interactions. Proc Natl Acad Sci U S A. 1999; 96:7731–7736. [PubMed: 10393889]

McHaffie JG, Beninato M, Stein BE, Spencer RF. Postnatal development of acetylcholinesterase in, cholinergic projections to, the cat superior colliculus. J Comp Neurol. 1991; 313:113–131. [PubMed: 1761749]

Morgan MM, Fossum EN, Levine CS, Ingram SL. Antinociceptive tolerance revealed by cumulative intracranial microinjections of morphine into the periaqueductal gray in the rat. Pharmacol Biochem Behav. 2006; 85:214–219. [PubMed: 16979226]

Morgan MM, Whitney PK, Gold MS. Immobility and flight associated with antinociception produced by activation of the ventral and lateral/dorsal regions of the rat periaqueductal gray. Brain Res. 1998; 804:159–166. [PubMed: 9729359]

Morris BJ, Simpson CS, Mundell S, Maceachern K, Johnston HM, Nolan AM. Dynamic changes in NADPH-diaphorase staining reflect activity of nitric oxide synthase: evidence for a dopaminergic regulation of striatal nitric oxide release. Neuropharmacology. 1997; 36:1589–1599. [PubMed: 9517430]

Nandi R, Fitzgerald M. Opioid analgesia in the newborn. Eur J Pain. 2005; 9:105–108. [PubMed: 15737795]

Oakman SA, Faris PL, Kerr PE, Cozzari C, Hartman BK. Distribution of pontomesencephalic cholinergic neurons projecting to substantia nigra differs significantly from those projecting to ventral tegmental area. J Neurosci. 1995; 15:5859–5869. [PubMed: 7666171]

Okere CO, Waterhouse BD. Activity-dependent heterogeneous populations of nitric oxide synthase neurons in the rat dorsal raphe nucleus. Brain Res. 2006a; 1086:117–132. [PubMed: 16616732]

Okere CO, Waterhouse BD. Acute capsaicin injection increases nicotinamide adenine dinucleotide phosphate diaphorase staining independent of Fos activation in the rat dorsolateral periaqueductal gray. Neurosci Lett. 2006b; 404:288–293. [PubMed: 16835009]

Okere CO, Waterhouse BD. Acute restraint increases NADPH-diaphorase staining in distinct subregions of the rat dorsal raphe nucleus: implications for raphe serotonergic and nitrergic transmission. Brain Res. 2006c; 1119:174–181. [PubMed: 16989783]

Onstott D, Mayer B, Beitz AJ. Nitric oxide synthase immunoreactive neurons anatomically define a longitudinal dorsolateral column within the midbrain periaqueductal gray of the rat: analysis using laser confocal microscopy. Brain Res. 1993; 610:317–324. [PubMed: 7686435]

Paxinos, G.; Watson, C. The rat brain in stereotaxic coordinates. Orlando, FL: Academic Press; 1998.

Rahman W, Dickenson AH. Development of spinal opioid systems. Reg Anesth Pain Med. 1999; 24:383–385. [PubMed: 10499746]

Rodrigo J, Springall DR, Uttenthal O, Bentura ML, Abadia-Molina F, Riveros-Moreno V, Martinez-Murillo R, Polak JM, Moncada S. Localization of nitric oxide synthase in the adult rat brain. Philos Trans R Soc Lond B Biol Sci. 1994; 345:175–221. [PubMed: 7526408]

Shin JH, Chung S, Park EJ, Uhm DY, Suh CK. Nitric oxide directly activates calcium-activated potassium channels from rat brain reconstituted into planar lipid bilayer. FEBS Lett. 1997; 415:299–302. [PubMed: 9357987]

Simpson KL, Waterhouse BD, Lin RC. Differential expression of nitric oxide in serotonergic projection neurons: neurochemical identification of dorsal raphe inputs to rodent trigeminal somatosensory targets. J Comp Neurol. 2003; 466:495–512. [PubMed: 14566945]

Siuciak JA, Advokat C. Tolerance to morphine microinjections in the periaqueductal gray (PAG) induces tolerance to systemic, but not intrathecal morphine. Brain Res. 1987; 424:311–319. [PubMed: 3676830]

Spessert R, Layes E. Fixation conditions affect the intensity but not the pattern of NADPH-diaphorase staining as a marker for neuronal nitric oxide synthase in rat olfactory bulb. J Histochem Cytochem. 1994; 42:1309–1315. [PubMed: 7523486]

Sugaya K, McKinney M. Nitric oxide synthase gene expression in cholinergic neurons in the rat brain examined by combined immunocytochemistry and in situ hybridization histochemistry. Brain Res Mol Brain Res. 1994; 23:111–125. [PubMed: 7518028]

Takeya R, Ueno N, Kami K, Taura M, Kohjima M, Izaki T, Nunoi H, Sumimoto H. Novel human homologues of p47phox and p67phox participate in activation of superoxide-producing NADPH oxidases. J Biol Chem. 2003; 278:25234–25246. [PubMed: 12716910]

Thornton SR, Smith FL. Characterization of neonatal rat fentanyl tolerance and dependence. J Pharmacol Exp Ther. 1997; 281:514–521. [PubMed: 9103539]

Thornton SR, Wang AF, Smith FL. Characterization of neonatal rat morphine tolerance and dependence. Eur J Pharmacol. 1997; 340:161–167. [PubMed: 9537810]

Tive LA, Barr GA. Analgesia from the periaqueductal gray in the developing rat: focal injections of morphine or glutamate and effects of intrathecal injection of methysergide or phentolamine. Brain Res. 1992; 584:92–109. [PubMed: 1355395]

Tortorici V, Morgan MM, Vanegas H. Tolerance to repeated microinjection of morphine into the periaqueductal gray is associated with changes in the behavior of off- and on-cells in the rostral ventromedial medulla of rats. Pain. 2001; 89:237–244. [PubMed: 11166480]

Tortorici V, Robbins CS, Morgan MM. Tolerance to the antinociceptive effect of morphine microinjections into the ventral but not lateral-dorsal periaqueductal gray of the rat. Behav Neurosci. 1999; 113:833–839. [PubMed: 10495091]

Tseng LF, Collins KA, Wang Q. Differential ontogenesis of thermal and mechanical antinociception induced by morphine and beta-endorphin. Eur J Pharmacol. 1995; 277:71–76. [PubMed: 7635176]

Usunoff KG, Kharazia VN, Valtschanoff JG, Schmidt HH, Weinberg RJ. Nitric oxide synthase-containing projections to the ventrobasal thalamus in the rat. Anat Embryol (Berl). 1999; 200:265–281. [PubMed: 10463342]

van der Veen BS, de Winther MP, Heeringa P. Myeloperoxidase: molecular mechanisms of action and their relevance to human health and disease. Antioxid Redox Signal. 2009; 11:2899–2937. [PubMed: 19622015]

von Lohneysen K, Noack D, Jesaitis AJ, Dinauer MC, Knaus UG. Mutational analysis reveals distinct features of the Nox4-p22 phox complex. J Biol Chem. 2008; 283:35273–35282. [PubMed: 18849343]

Xu JY, Hill KP, Bidlack JM. The nitric oxide/cyclic GMP system at the supraspinal site is involved in the development of acute morphine antinociceptive tolerance. J Pharmacol Exp Ther. 1998; 284:196–201. [PubMed: 9435178]

Xu ZQ, Hokfelt T. Expression of galanin and nitric oxide synthase in subpopulations of serotonin neurons of the rat dorsal raphe nucleus. J Chem Neuroanat. 1997; 13:169–187. [PubMed: 9315967]

Yang Q, Chen SR, Li DP, Pan HL. Kv1.1/1.2 channels are downstream effectors of nitric oxide on synaptic GABA release to preautonomic neurons in the paraventricular nucleus. Neuroscience. 2007; 149:315–327. [PubMed: 17869444]

Zhu H, Barr GA. Inhibition of morphine withdrawal by the NMDA receptor antagonist MK-801 in rat is age-dependent. Synapse. 2001a; 40:282–293. [PubMed: 11309844]

Zhu H, Barr GA. Opiate withdrawal during development: are NMDA receptors indispensable? Trends Pharmacol Sci. 2001b; 22:404–408. [PubMed: 11479002]

Zhu H, Barr GA. Ontogeny of NMDA receptor-mediated morphine tolerance in the postnatal rat. Pain. 2003; 104:437–447. [PubMed: 12927616]

HIGHLIGHTS

- Acute morphine activates Fos in the ventral PAG in both adult and newborn rat at PD7.
- This effect was attenuated after chronic morphine administration in both adult and PD7 rat.
- In adult but not PD7 rats, nitric oxide is implicated in mediation of chronic morphine effects.
- Gene expression suggests superoxide and hydrogen peroxide mechanisms in PD7 rats.
- Oxidative stress pathways associated with chronic morphine exposure are age-specific.

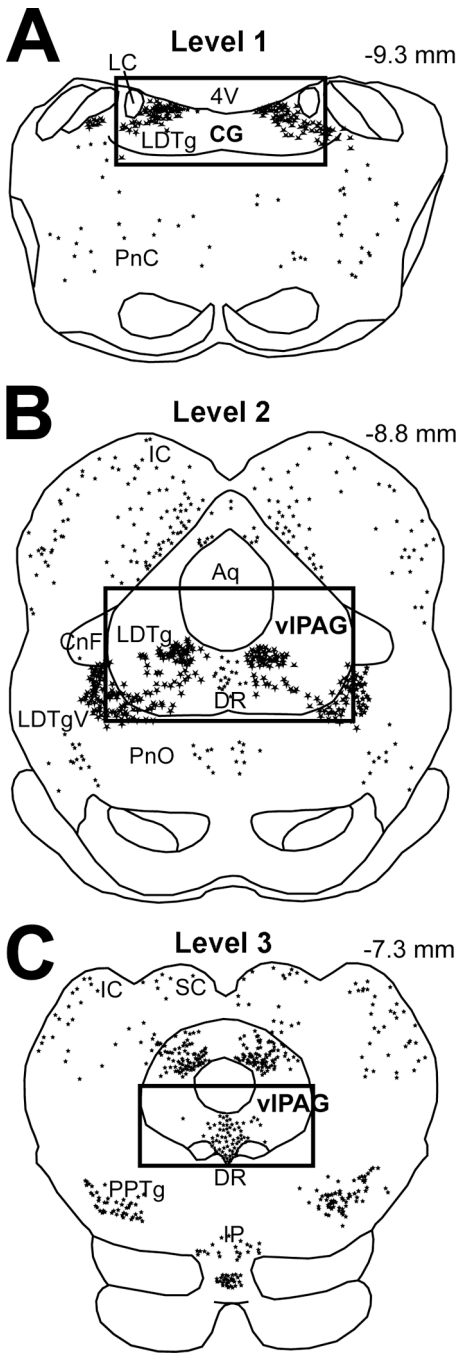

Figure 1. Schematic Representation of Areas of Analysis

Schematic drawings of adult rat brain coronal brainstem sections illustrate distribution of neuronal nitric oxide synthase (nNOS) immunoreactive neurons that are represented as stars. Differences in star size reflect differences in the size of individual nNOS neurons. Anatomical areas of analysis are marked by a square: **(A) Level 1** encompasses the central gray (CG) at the level of the rostral locus coeruleus (LC; corresponding to plates 56–59 of the adult rat brain atlas (Paxinos and Watson, 1998)), **(B) Level 2** includes the ventrolateral periaqueductal gray (vlPAG) at the level of the inferior colliculus (IC) (corresponding to Plates 53–55), and **(C) Level 3** includes the vlPAG at the level of the superior colliculus

(SC) (corresponding to Plates 48–52). Large nNOS immunoreactive neurons are located within the laterodorsal tegmental nucleus (LDTg) at levels 1 and 2. ***Abbreviations***: **4V**, fourth ventricle; **Aq**, aqueduct (Sylvius); **CnF**, cuneiform nucleus; **DR**, dorsal raphe nucleus; **IP**, interpeduncular nucleus; **LDTgV**; laterodorsal tegmental nucleus, ventral part; **PnC**; pontine reticular nucleus, caudal part; **PnO**, pontine reticular nucleus, oral part; **PPTg**, pedunculopontine tegmental nucleus. Numbers in the upper right corner represent distance from Bregma.

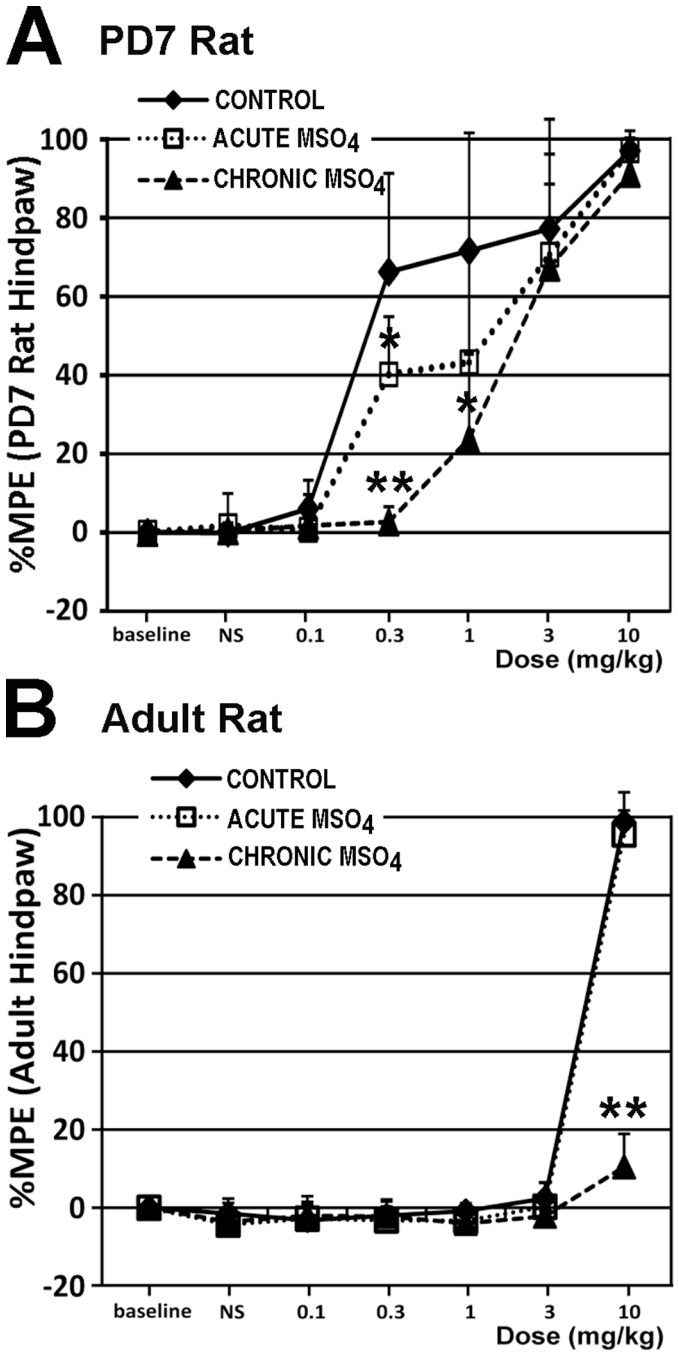

Figure 2. Behavioral Analysis of Morphine Antinociceptive Effects

Hot Plate testing was done on the 7th day of treatment to evaluate development of antinociceptive tolerance (n=6/pharmacological group/age, except for n=7 for chronic morphine group in postnatal day (PD)7 rat). We used 49°C (with 20 s cutoff latency) for PD7 rats, and 56°C (with 12 s cutoff latency) for adult rats. Thus, morphine potency cannot be compared between two age groups. Chronic morphine treatment rendered both the the PD7 (F(2,16)=24.74; p<0.001 at 0.3 mg/kg testing dose) and adult rat (F(2,15)=228.9; p<0.001 at 10 mg/kg testing dose) tolerant to morphine's antinociceptive effects. Results are presented as a percentage of maximum possible effect (**%MPE** ± SD) according to the method of Harris and Pierson (Harris and Pierson, 1964) to construct dose-response curves

for morphine's antinociceptive effect. **Panel A**: In the PD7 rat, a morphine dose of 0.3 mg/kg showed evidence of tolerance development in the chronic morphine group (%MPE= 2.67± 3.87), in comparison to both control (66.24% ± 25.08; $p<0.01$) and acute morphine (40.19% ± 14.68; $p<0.01$) groups. Interestingly, the same morphine dose of 0.3 mg/kg led to a statistically significant decrease in %MPE of the acute morphine group versus control group ($p<0.05$), suggesting that even a single prior exposure to morphine attenuates its antinociceptive effect at this early age. Furthermore, a 1 mg/kg morphine test dose led to a statistically significant difference ($F(2,16)=5.17$; $p=0.01$) only between the control and chronic morphine group ($p<0.05$). **Panel B**: In the adult rat, a morphine dose of 10 mg/kg led to significantly lower %MPE in the chronic morphine group (10.46% ± 8.45), in comparison to control (98.81% ± 2.91; $p<0.01$) and acute morphine (95.58% ± 10.8; $p<0.01$) groups. ***Abbreviations:*** MSO_4, morphine; ******, $p<0.01$; *****, $p<0.05$.

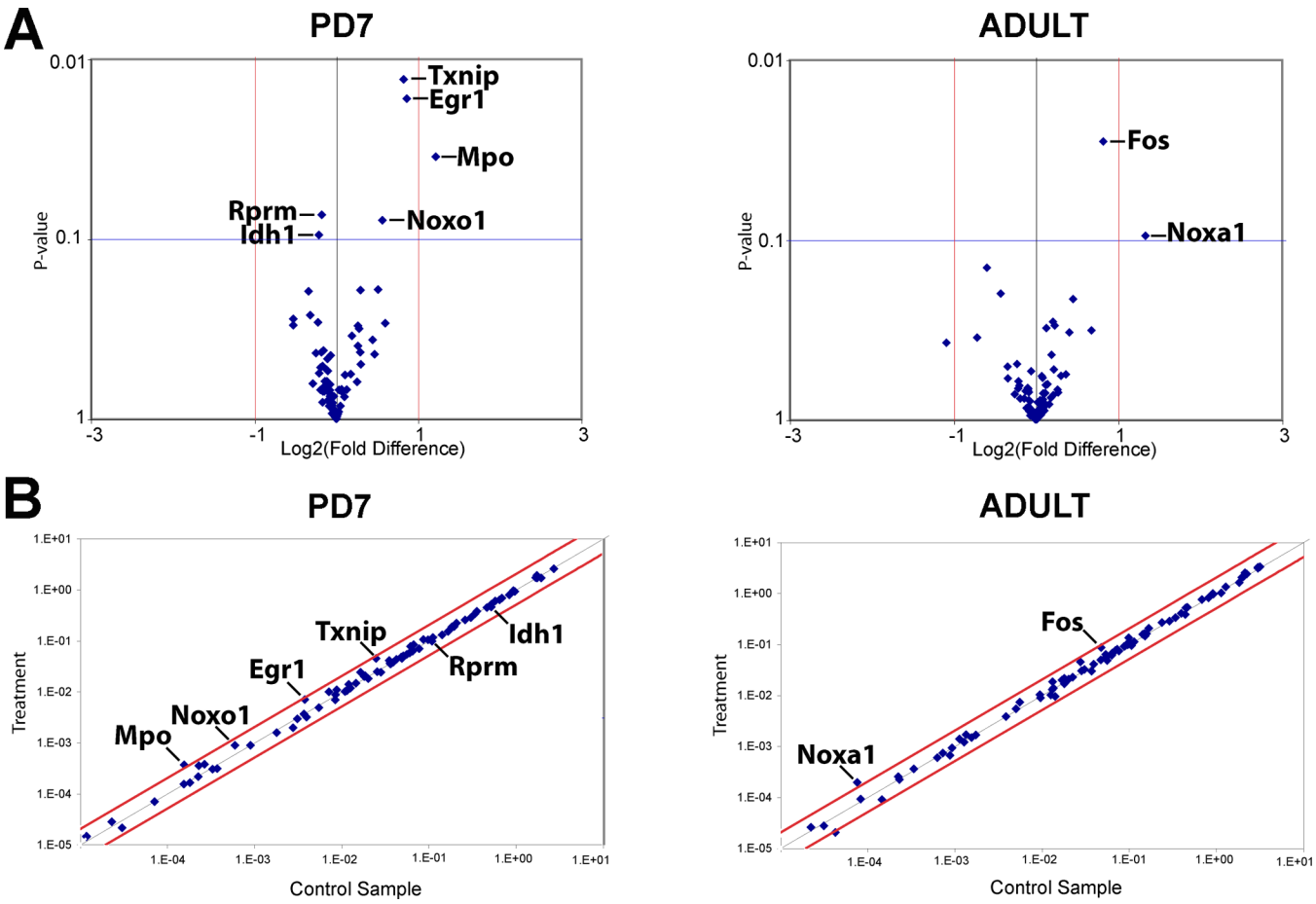

Figure 3. Gene Expression Analysis at the Ventral Periaqueductal Gray

Total of 84 genes were assayed using *Rat Nitric Oxide Signaling Pathway PCR Array* (PARN-062; SABiosciences™) in in the ventral periaqueductal gray at the level of the inferior colliculus (see also Fig. 1B). Gene expression was compared between treatment (chronic morphine) and control (chronic normal saline administration) at two different ages of the rat: postnatal day (PD)7 and adult. **(A) Volcano plots** illustrate relationship between the gene expression fold change and p-value for all the morphine tolerant and control pairs. Those with $p < 0.1$ for treatment effect are indicated. **(B) Scatter plots** for all of the genes assayed illustrating the relative abundance in control and chronic morphine treated conditions. X and Y axis in **Panel B** correspond to 2^-ΔCt [Ct(gene of interest)-Avg Ct (housekeeping gene, HKG]. ***Abbreviations*** of genes: ***Egr1***, Early growth response 1; ***Fos***, FBJ osteosarcoma oncogene; ***Idh1***, isocitrate dehydrogenase 1 (NADP+), soluble; ***MPO***, myeloperoxidase; ***Noxa1***, NADPH oxidase activator 1; ***Noxo1***, NADPH oxidase organizer 1; ***Txnip***, thioredoxin interacting protein.

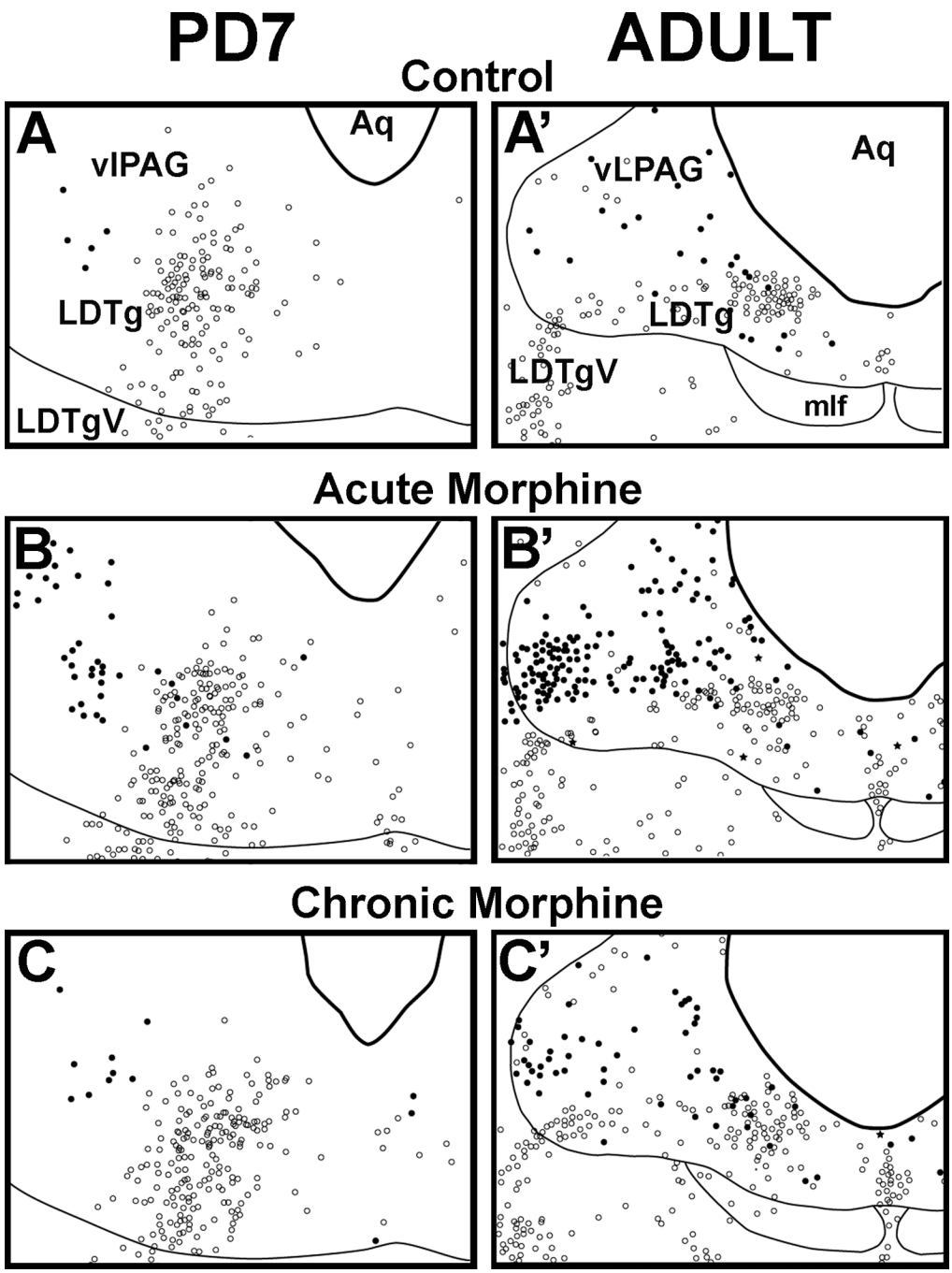

Figure 4. Anatomical Distribution of Fos-Immunoreactive Nuclei and nNOS-Immunoreactive Neurons in the Rostral Brainstem in PD7 and Adult Rats

Schematic drawings illustrate distribution of Fos and nNOS immunolabeling following normal saline (control, **A and A'**), acute morphine (**B and B'**), and chronic morphine treatments (**C and C'**) at the ventrolateral periaqueductal gray (vlPAG) at the level of the inferior colliculus (see also Fig. 1B; Level 2). Distribution of Fos nuclei and nNOS neurons is represented as black dots and open circles, respectively. Very few double-labeled neurons were labeled as black stars. Fine lines mark some anatomical landmarks. ***Abbreviations***: **Aq**, cerebral aqueduct; **LDTg**, laterodorsal tegmental nucleus; **LDTgV**; laterodorsal tegmental nucleus, ventral part; **mlf**, medial longitudinal fasciculus.

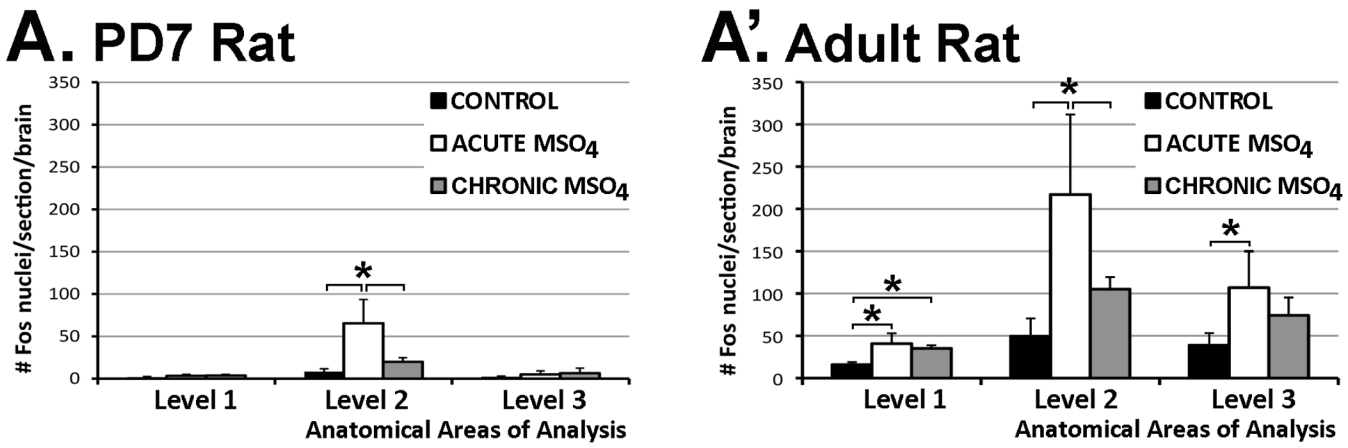

Figure 5. Distribution and Density of Fos Immunolabeling with Morphine Treatment

Graphs show average density (#Fos/section/brain ± SD) of Fos-immunoreactive nuclei following different pharmacological treatments: control, acute morphine, and chronic morphine administration in (**A**) PD7 and (**A'**) the adult rat. Three different brain regions were analyzed (shown in Fig. 1). **Panel A:** In the PD7 rat, statistically significant differences in Fos density among treatments are found only at Level 2 of the vlPAG at the inferior colliculus ($F(2,12)=16.82$; $p<0.001$) with a significant effect of acute morphine treatment on the number of Fos nuclei when compared to both the control ($p<0.01$) and chronic morphine group ($p<0.01$). No changes were found either caudally (Level 1; $F(2,9)=2.09$; $p=0.179$) or rostrally (Level 3; $F(2,10)=1.06$; $p=0.382$). **Panel A':** In the adult rat, statistically significant differences in estimated density among three different experimental groups were found in all three anatomical regions of analysis: Level 1 ($F(2,12)=14.96$; $p<0.001$), Level 2 ($F(2,12)=11.41$; $p<0.01$), and Level 3 ($F(2,12)=7.04$; $p<0.01$). At Level 1, density of Fos-immunoreactive nuclei was significantly higher between both acute and chronic morphine groups in comparison to control ($p<0.01$), but there were no differences between acute and chronic morphine groups. At Level 2, we showed significant increase in estimated density of Fos nuclei in the acute morphine group in comparison to both control ($p<0.01$) and chronic morphine groups ($p<0.05$). At Level 3, the acute morphine group was only different from control ($p<0.01$) but not from the chronic morphine group.

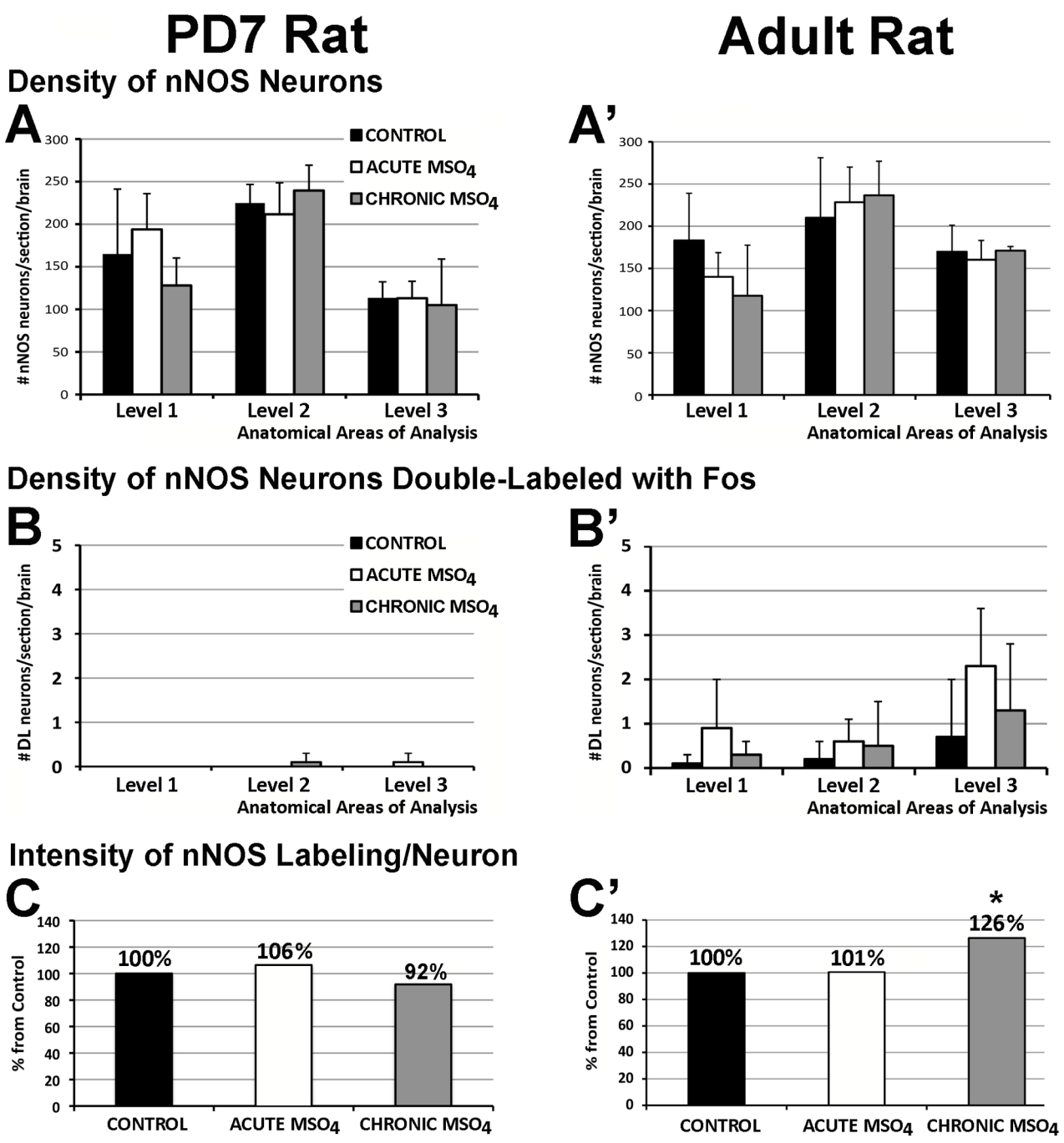

Figure 6. Density of Neuronal Nitric Oxide Synthase (nNOS) Neurons in Ventral Periaqueductal Gray with Pharmacological Treatment

Graphs in **Panels A and A'** show average density (#profiles/section/brain ± SD) of nNOS immunoreactive neurons, while **Panels B and B'** show average density of nNOS neurons double-labeled (DL) with Fos following different pharmacological treatment: control, acute morphine, and chronic morphine both in the PD7 (**A and B**) and the adult rat (**A' and B'**). There was no statistically significant difference in density of nNOS neurons in different anatomical regions following different pharmacological treatment for either PD7 or adult rat. Very few double-labeled neurons (nNOS neurons with Fos nuclei) were identified in the adult rat that did not change among the different treatment groups. Double-labeling in the

PD7 rat was negligible. **(C and C') Average intensity of nNOS immunolabeling per individual neuron in the cluster of nNOS immunoreactive neurons with treatment.** Region of analysis included nNOS neurons at inferior colliculus (shown in Fig. 1B) of PD7 and the adult rat. No changes were found in PD7 rats among different treatment ($F(2, 12)=0.59$, $p=0.57$; **C**). In the adult rat, percent (%) increase from control of average intensity of nNOS immunoreactive labeling per neuron in chronic morphine group was significantly increased (26%; $F(2,15)=10.4$; $p=0.001$; **C'**) when compared to control ($p=0.02$) and acute morphine groups ($p=0.02$). Asterisk (*****) indicates $p<0.05$, significant difference.

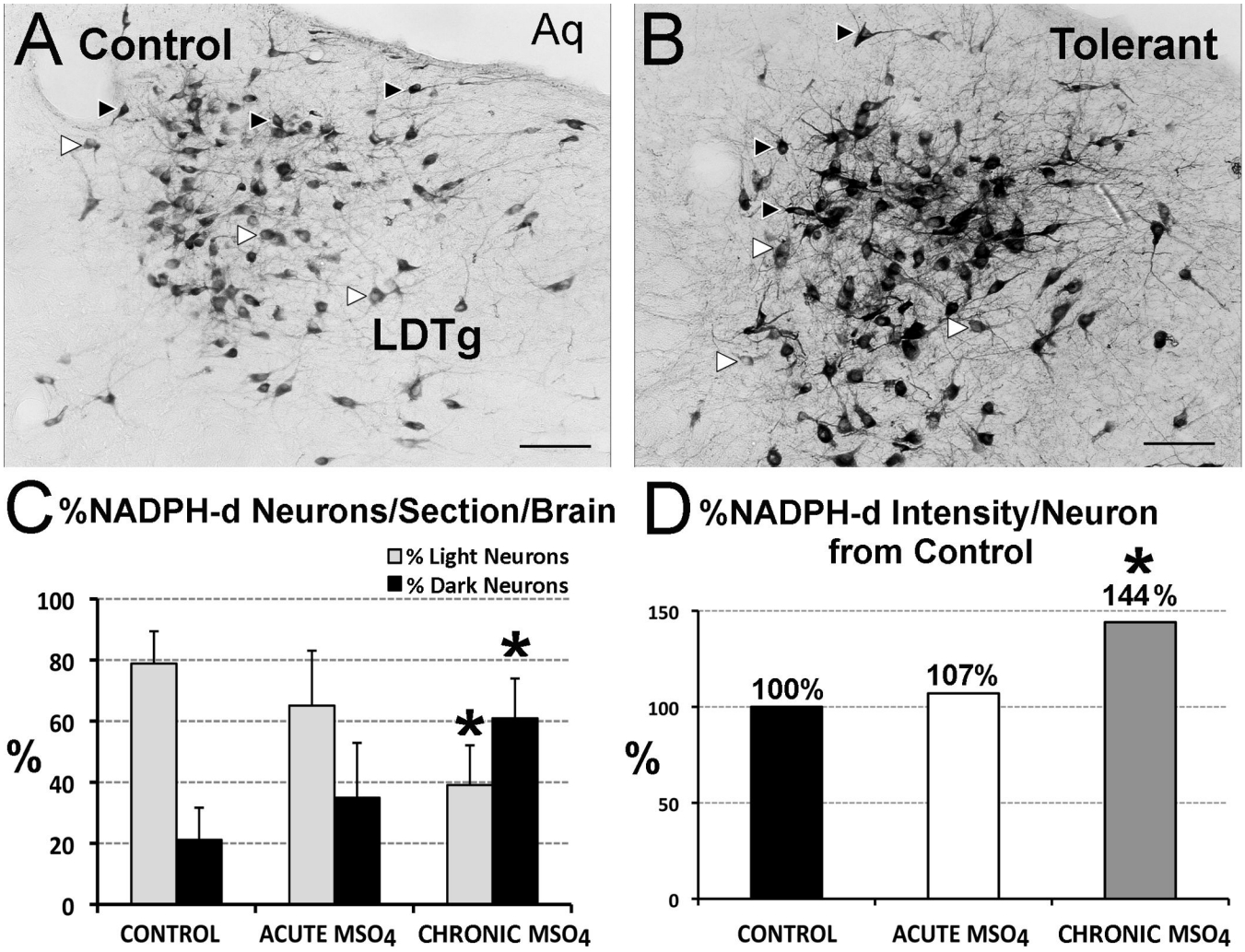

Figure 7. NADPH-d Histochemistry Reaction of the Adult Rat

Representative images of NADPH-d staining in the laterodorsal tegmental nucleus (LDTg) in adult rats treated with chronic injections of normal saline (control; **A**) versus chronic morphine (tolerant; **B**). Examples of lightly labeled neurons are marked with white arrow, while dark ones are indicated with black arrows. Total number of labeled NADPH-d neurons per brain across the LDTg is unchanged among different pharmacological groups (n=6/group; $F(2,15)=1.79$; p=0.2). **Panel C** illustrates that the percent (%) of intensely labeled (dark) NADPH-d neurons/section/brain was significantly higher in the chronic morphine group ($F(2,15)=11.39$, $p<0.001$; 60.18% ± 12.49) in comparison to both control (21.64% ± 11.25; $p<0.01$) and acute morphine (34.91% ± 17.97; $p<0.05$) groups, while the % of lightly labeled NADPH-d neurons/section/brain was significantly lower in chronic morphine group ($F(2,15)=11.96$, $p<0.001$; 39.83% ± 12.49) in comparison to both control (78.86% ± 10.53; $p<0.01$) and acute morphine (65.09% ± 17.97; $p<0.05$) groups. **Panel D** shows significant changes in percent intensity of NADPH-d reaction per individual neuron in the adult LDTg between the three treatment groups ($F(2,15)=13.45$; $p<0.001$). Specifically, the average intensity of NADPH-d reaction per individual adult neuron of LDTg increased by 44% in the group that received chronic morphine treatment compared to control ($p<0.01$) and acute morphine ($p<0.01$) groups. Scale bar = 100 μm. ***Abbreviations***:

Aq, cerebral aqueduct; **NADPH-d**, nicotinamide adenine dinucleotide phosphate diaphorase; *****, significant difference.